CONF-790847--1

LA-UR -79-2046

TITLE: SEARCH FOR PARITY-VIOLATING CONTRIBUTIONS TO SCATTERING OF HADRONS

AUTHOR(S): J. Ziskind, V. Yuan, R. Mischke, J. Potter, D. Nagle, D. Bowman, C. Hoffman, P. Chamberlain, H. Frauenfelder, C. Barnes, R. Talaga, and R. Carlini

SUBMITTED TO: International Conference on High Energy Physics and Nuclear Structure, Vancouver, Canada, August 13-17, 1979.

MASTER

University of California

LOS ALAMOS SCIENTIFIC LABORATORY
Post Office Box 1663 Los Alamos, New Mexico 87545
An Affirmative Action/Equal Opportunity Employer

J. Ziskind, Cal Tech

V. Yuan

R. Mischke

J. Potter

D. Nagle

D. Bowman

C. Hoffman

P. Chamberlain, MP-12/816

H. Frauenfelder, U. of Ill.

C. Barnes, Cal Tech

R, Talaga

R. Carlini

SEARCH FOR PARITY-VIOLATING CONTRIBUTIONS TO SCATTERING OF HADRONS

LASL, California Institute of Technology, University of Illinois

ABSTRACT

The study of parity violation is, at present, the only means of studing the weak nonleptonic strangness conserving nucleon-nucleon force at medium energies. The experiment is a search for parity nonconservation in P-Nucleus scattering by observing a change in the total cross section as the helicity of the incident protons is reversed. A non-vanishing helicity dependent cross section,

$$A= \frac{\sigma_+ - \sigma_-}{\sigma_+ + \sigma_-}$$

would imply the presence of a parity-violating interaction. The experiment utilized the 800-MeV longitudinally polarized external proton beam at the Clinton P. Anderson Meson Physics Facility of the Los Alamos Scientific Laboratory.

The result of the most recent run, March 1979, is as follows: no parity violation is observed:

$$A= -2.5 \pm 3.2 \times 10^{-6}$$

The systematic error contributions are not greater than 0.5×10^{-6}.

SEARCH FOR PARITY-VIOLATING CONTRIBUTION TO SCATTERING OF HADRONS

LASL, California Institute of Technology, University of Illinois

The experiment is a search for parity nonconservation in p-nucleus scattering by observing a change in the total cross section as the helicity of the incident protons is reversed. A nonvanishing helicity dependence would imply the presence of a parity-violating interaction. Recent calculations[1,2] based on models of the weak force between nucleons predict the helicity-dependent cross section,

$$A = \frac{\sigma_+ - \sigma_-}{\sigma_+ + \sigma_-} \quad ,$$

for p-p scattering to be at the level of a few parts in 10^{-7}. The experiment utilized the 800-MeV longitudinally polarized external proton beam at LAMPF.

Experiments were conducted over an 18-day period during the last quarter of 1978 and again for 14 days during March 1979. The work performed during the final quarter of 1978 concentrated on continuing studies of our ion-chamber detector characteristics and on the initial implementation of beam control servosystems. In addition, the random noise spectrum of the beam was measured and is plotted in Fig. 1. The results were subsequently used as a basis for choosing the 30-Hz polarization reversal frequency selected for the March 1979 data run. Also completed were extensive refinements and testing of our electronics and data-acquisition system.

During March 1979 a longitudinally polarized beam averaging 1 nA in intensity was utilized in conjunction with a 25-cm CH_2 target to perform our first attempt at measuring the p-CH_2 helicity-dependent cross section. Upper limits on systematic errors were determined. Preliminary analysis of the data indicates the cross-section asymmetry is consistent with zero at the 10^{-6} level.

The p-CH_2 cross-section asymmetry was determined by measuring the transmission of a longitudinally polarized proton beam with ion chambers placed on either side of the target, as illustrated in Fig. 2. The asymmetry is related to transmission T and longitudinal polarization P

$$A = \frac{1}{P\ell nT} \times \frac{(T_+ - T_-)}{2T}$$

where the subscripts indicate the helicity of incident protons. The helicity was reversed rapidly to minimize systematic errors caused by beam motion and electronics-related drifts. We decided to reverse the helicity at 30 Hz, a frequency wherein the beam-intensity fluctuations are minimal, as shown in Fig 1.

Because A is a very small quantity, it is important to monitor and control the various properties of the proton beam. Small changes in the beam intensity, position, or transverse polarization will alter the transmission measurement and cause errors in determining A. More important, if these changes occur in phase with helicity reversal, a spurious cross-section asymmetry will result. It is a major thrust of the experiment to stabilize the beam properties such that any spurious signal be suppressed well below the accuracy of the measured asymmetry.

Beam position was stabilized using feedback from the split-plate ion chamber (see Fig. 2) to a steering magnet. Vertical and horizontal residual polarizations were minimized using feedback from the split-scintillator polarimeter to drive correction magnets in the argon cell of the polarized proton source. Changes in beam intensity were also minimized with feedback from the ion chamber upstream of the target to a quenching electrode in the source. Both polarization and intensity feedbacks were driven by lock-in amplifiers tuned to the 30-Hz reversal frequency.

We quantify the possible systematic errors according to a simple model. Various properties beside helicity are carried by beam, and can have a time variation with a Fourier component at the spin-reversal frequency. They can produce in the detector a spurious parity violation signal. Properties which have been identified are: Intensity Modulation (IMOD), Horizontal Polarization (HPOL), Vertical Polarization (VPOL), and Horizontal and Vertical Position Modulation (HPOS) and (VPOS). The measured asymmetry, A_m, is related to the actual asymmetry, A,

$$A_m = A + \alpha_1 \mathrm{IMOD} + \alpha_2 \mathrm{HPOS} + \alpha_3 \mathrm{VPOS} + \alpha_4 \mathrm{HPOL}(Y - Y_0) + \alpha_5 \mathrm{VPOL}(X - X_0)$$

where Y and X are respectively the vertical and horizontal displacements of the beam centroid from Y_0 and X_0. The 30-Hz component of each of those beam properties was measured and every effort was made to reduce its magnitude.

The remaining value of each property is called the "residual." The detector systems are designed and adjusted to have these quantities produce a minimal effect on the transmission. These effects, or detector sensitivities, are defined, for example, as $\partial A/\partial(\mathrm{IMOD}) = \alpha_1$, the sensitivity of the parity-violation measurement to the intensity modulation of the beam and similarly for the other quantities listed in Table II. These sensitivities were determined by ancillary measurements many times in the course of a data-taking run. For instance, the magnitude of IMOD was increased several hundred times, resulting in a spurious signal at the 10^{-5} level. The phase of IMOD was reversed and resulted in a spurious signal of the opposite sign. The contribution of a particular systematic error is the product of its measured "sensitivity" with the corresponding "residual."

A successful search for a parity signal at the level of 10^{-6} required reducing the geometric sum of all beam-dependent and electronics-introduced errors to better than one part in 10^6. To control electronically introduced errors, much effort was expended in the design of special electronics. In many cases we were required to deal with sources of error that normally are not a problem, but which become significant in a measurement at this level of precision. An example of this kind of problem is truncation error, an error introduced in reading the voltage to frequency converters (V/f) at the 120-Hz beam pulse rate, and which became significant at the 10^{-6} level in the first version of our data-acquisition system. The system was accordingly redesigned and improved using new techniques described below.

It became evident that the 500-μs integration time caused inaccuracy in the digitization because the maximum frequency of V/f devices is 10^6 Hz. The small number of pulses generated during each beam macropulse was subject to a truncation error that appears at the 10^{-6} level. We devised two alternate ways to circumvent this problem. In one method we reduced the truncation error by defining a new beam gate which was determined by the first and last digitization pulses. The length of this new variable gate was monitored with a precision, high-frequency clock. The other method to reduce truncation error was to take an analog difference between signals from IC1 and IC2. The IC2 signal level was adjusted to match that of IC1. The difference, normalized by IC1 signal, was then amplified and fed to a V/f device. The truncation error was reduced by that amplification factor.

Prior to the March data runs, tests were performed utilizing current sources to simulate the detector (ion chamber) output. These tests indicate that electronic and digital errors (including truncation error) are now being controlled to a level of a few parts in 10^{-8}. This effect is a contribution to the noise, not a systematic error.

Servoloops were employed in the control of beam motion, reducing slow position drifts by better than an order of magnitude. The 60-Hz component of beam motion was also effectively controlled. These systems have proven effective for other users on EPB.

It was important to construct the ion chambers so that their response characteristics were very similar to each other. Such common response minimized contributions from slight nonlinearities in the relation between beam flux and ionization current. With this in mind, a pair of ion chambers were constructed to be identical to a high mechanical tolerance. High electric fields were used to minimize space-charge effects and electron-ion recombination. Hydrogen gas was used to take advantage of the high mobility of its ions. In addition, the low electron density of hydrogen gas minimized space-charge build-up. Care was taken to maintain purity of the gas.

The preliminary results, as tabulated in Table I, indicate $A = (-2.5 \pm 3.2) \times 10^{-6}$. Shown in Table II is a summary of the measured "sensitivities" and "residuals" along with calculated limits of their contributions to the cross-section asymmetry. The geometric sum of these contributions is significantly less than the measured accuracy of the cross-section asymmetry.

We are now studying ways to further improve our beam control methods and detector sensitivities, to a level of 10^{-7}, where present theoretical predictions indicate a parity violation can be expected. In the future we will decrease the magnitude of the "residuals" and any significant contributions to A will be measured and subtracted. A liquid-hydrogen target is being designed for this experiment. Additional servoloops are planned for controlling the 30Hz position modulation components in the beam.

Other improvements are in the performance of the Lamb Shift Ion Source, particularly in its stability and intensity. Extensive test runs in April by MP-12 have shown that we may expect 10 nA in July, and further improvements later. Such an increase will improve the experiment in two ways. First, the fluctuations of the beam characteristics, or "residuals," can be controlled better because of the greater signal-to-noise ratio in the feedback loops. The result will be reduced systematic errors. Second, the statistical fluctuations of proton-nucleus scattering will decrease.

A further run is planned in July to test methods of controlling the errors to the next level of sensitivity.

REFERENCES

1. E. M. Henley and F. R. Krejs, Phys. Rev. D11, 605 (1975).
2. J. D. Bjorken, private communication of informal calculation, 1978.

TABLE I

Target Material	Polarization Status	Helicity-Dependent Cross Section
25 cm CH_2	Reversing 30 Hz	$(-2.5 \pm 3.2) \times 10^{-6}$
None	Reversing 30 Hz	$(-2.4 \pm 3.8) \times 10^{-6}$
25 cm CH_2	Nonreversing	$(-6.5 \pm 4.1) \times 10^{-6}$

TABLE II

Measured Sensitivities

Type	$A_{observed}$ Sensitivity	Residual	Contributions to $A_{observed}$ (Sensitivity x Residual)
$\frac{\partial A}{\partial(IMOD)}$	$(-155 \pm 27) \times 10^{-4}$	$(2.3 \pm .5) \times 10^{-5}$	$(3.6 \pm 1.0) \times 10^{-7}$
$\frac{\partial A}{\partial(IIPOL)}$	41×10^{-4}/cm	$\frac{(1.1 \pm 1.2) \times 10^{-5}}{(Y - Y_0)^*}$	$(.36 \pm .39) \times 10^{-7}$
$\frac{\partial A}{\partial(VPOL)}$	150×10^{-4}/cm	$\frac{(1.8 \pm 1.7) \times 10^{-5}}{(X - X_0)^{**}}$	$(2.1 \pm 2.0) \times 10^{-7}$
$\frac{\partial A}{\partial(IIPOS)}$	$(6.9 \pm .7) \times 10^{-4}$/cm	$(-.6 \pm 1.0) \times 10^{-4}$cm	$(-.4 \pm .67) \times 10^{-7}$
$\frac{\partial A}{\partial(VPOS)}$	$(6.9 \pm .7) \times 10^{-4}$/cm	$(-3.2 \pm .9) \times 10^{-4}$ cm	$(-2.2 \pm .66) \times 10^{-7}$

*$(Y - Y_0)$ = .8 cm

**$(X - X_0)$ = .8 cm

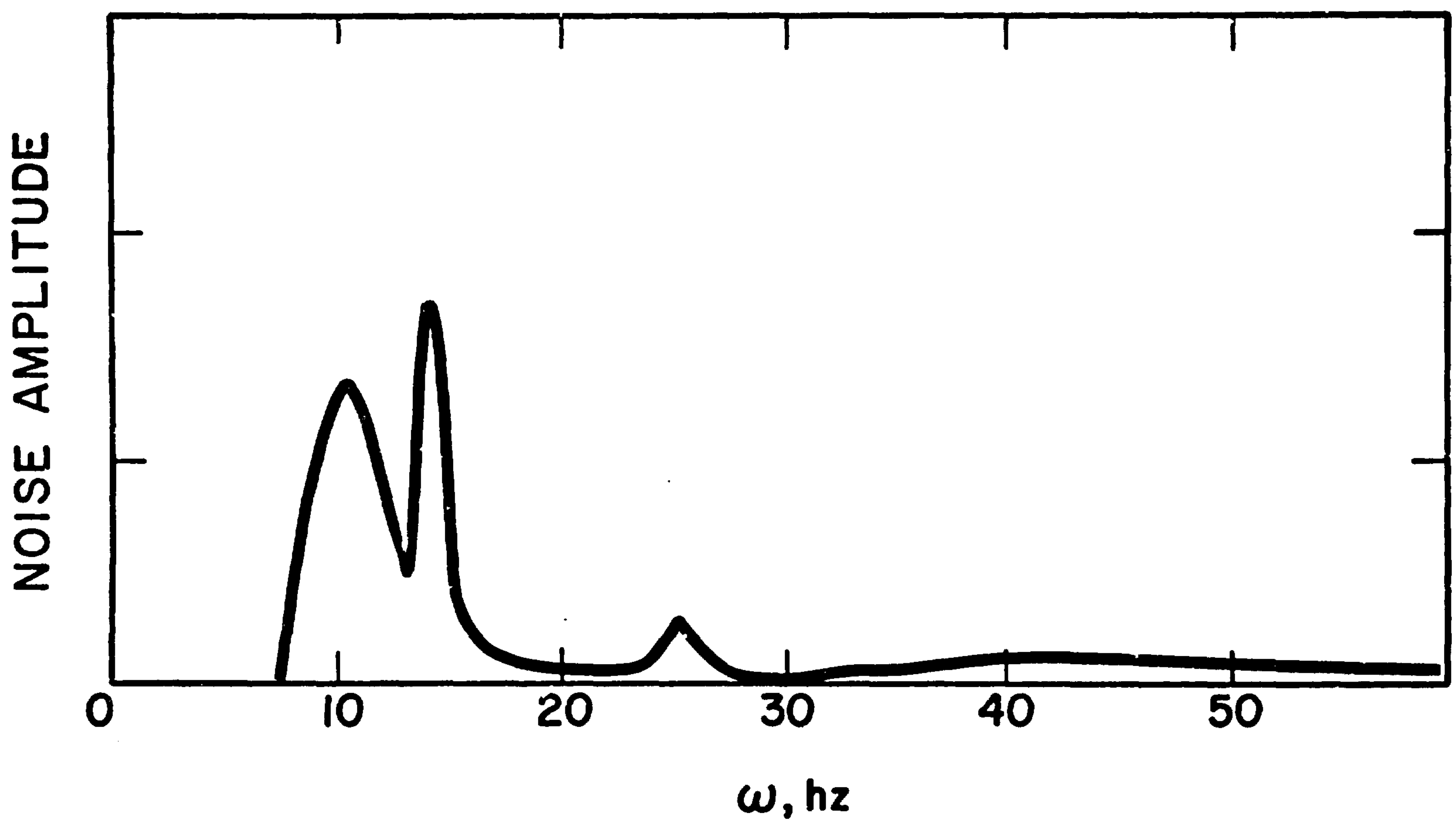

FIG. 1. NOISE SPECTRUM.

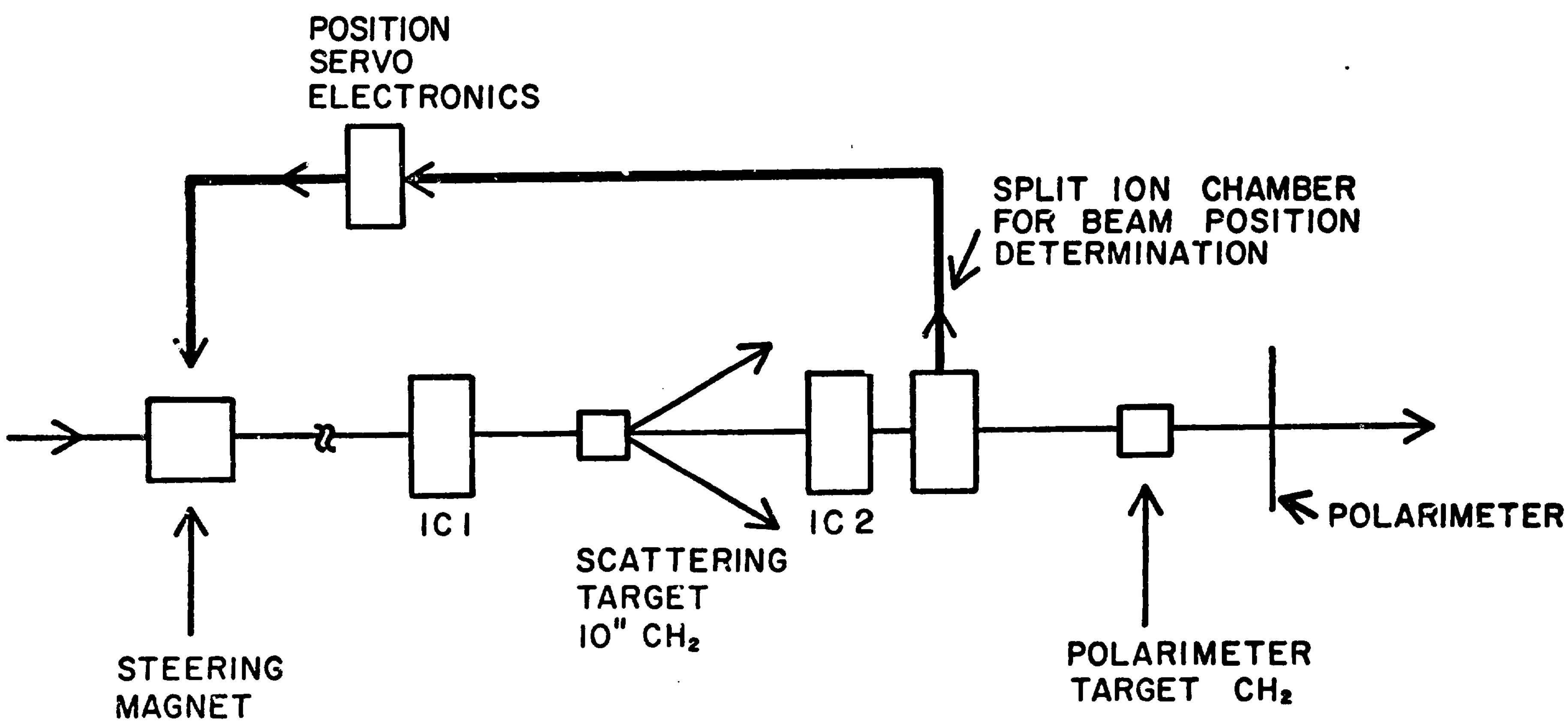

SCHEMATIC OF EXP. 137 APPARATUS

FIG. 2